The Astrophysical Journal, 604:339–345, 2004 March 20

PULSAR PARALLAXES AT 5 GHz WITH THE VERY LONG BASELINE ARRAY

S. Chatterjee,[1,2,3] J. M. Cordes,[1] W. H. T. Vlemmings,[1] Z. Arzoumanian,[4] W. M. Goss,[2] and T. J. W. Lazio[5]

Received 2003 October 7; accepted 2003 December 2

ABSTRACT

We present the first pulsar parallaxes measured with phase-referenced pulsar VLBI observations at 5 GHz. Because of the steep spectra of pulsars, previous astrometric measurements have been at lower frequencies. However, the strongest pulsars can be observed at 5 GHz, offering the benefit of lower combined ionospheric and tropospheric phase errors, which usually limit VLBI astrometric accuracy. The pulsars B0329+54, B0355+54, and B1929+10 were observed for seven epochs spread evenly over 2 years. For B0329+54, large systematic errors led to only an upper limit on the parallax ($\pi < 1.5$ mas). A new proper motion and parallax were measured for B0355+54 ($\pi = 0.91 \pm 0.16$ mas), implying a distance of $1.04^{+0.21}_{-0.16}$ kpc and a transverse velocity of 61^{+12}_{-9} km s^{-1}. The parallax and proper motion for B1929+10 were significantly improved ($\pi = 2.77 \pm 0.07$ mas), yielding a distance of 361^{+10}_{-8} pc and a transverse velocity of 177^{+4}_{-5} km s^{-1}. We demonstrate that the astrometric errors are correlated with the angular separation between the phase-reference calibrator and the target source, with significantly lower errors at 5 GHz as compared to 1.6 GHz. Finally, based on our new distance determinations for B1929+10 and B0355+54, we derive or constrain the luminosities of each pulsar at high energies. We show that, for thermal emission models, the emitting area for X-rays from PSR B1929+10 is roughly consistent with the canonical size for a heated polar cap and that the conversion of spin-down power to γ-ray luminosity in B0355+54 must be low. The new proper motion for B1929+10 also implies that its progenitor is unlikely to have been the binary companion of the runaway O star ζ Ophiuchi.

Subject headings: astrometry — pulsars: individual (PSR B0355+54, PSR B1929+10) — stars: kinematics — stars: neutron — X-rays: stars

1. INTRODUCTION

The measurement of distances is a fundamental problem in astronomy. Trigonometric parallax offers one of the only model-independent mechanisms for such measurements, thus defining the lowest rungs of the distance ladder. The parallaxes and proper motions of pulsars, obtained through imaging or pulse-timing observations, provide measurements of their distances and velocities, and thus allow us to probe the physics of neutron star formation in supernovae, as well as the intervening interstellar medium which scatters and disperses the radio pulses from pulsars.

Pulsar distances provide crucial calibration for electron density distribution models of the Galaxy (e.g., Taylor & Cordes 1993; Cordes & Lazio 2002), which in turn provide estimates of the distances to the majority of the pulsar population and underlie estimates of their velocities. The velocity distribution of pulsars (Arzoumanian, Chernoff, & Cordes 2002) helps constrain core collapse processes in supernovae (Burrows & Hayes 1996), while velocities of individual objects can be used to trace their progenitor supernovae and birth sites (Hoogerwerf, de Bruijne, & de Zeeuw 2001). Recent results from X-ray observations coupled with distance estimates have established constraints on neutron star cooling curves (Tsuruta et al. 2002) which limit plausible nuclear equations of state.

While the diverse applications of pulsar distances and velocities make a compelling case for the necessity of pulsar astrometry, reliable measurements have been few and far between (see, e.g., Toscano et al. 1999). The paucity of parallax measurements is due to the difficulty of measuring the effect. For a pulsar at 1 kpc, the angular displacement is only 1 mas and the semiannual timing perturbation is 1.6 μs. Few pulsars can be observed with sufficient precision to measure the timing effect, while astrometry with ad hoc very long baseline interferometry (VLBI) arrays has been difficult and inconsistent. However, the advent of the NRAO Very Long Baseline Array, a full-time, dedicated VLBI instrument, coupled with pulsar gating and refined calibration techniques, has significantly altered the situation and led to several parallax measurements in recent years (Brisken et al. 2000; Chatterjee et al. 2001; Brisken et al. 2002). Because of the steep spectra of pulsars ($S_\nu \propto \nu^\alpha$, $\langle \alpha \rangle \sim -1.6$; Lorimer et al. 1995), these measurements have all been at 1.4 GHz, a frequency lower than that used for most other VLBI astrometry. Here we present the first pulsar parallaxes measured at 5 GHz. In § 2, we outline the observations, calibration process, and data analysis. Astrometric results for the pulsars B0329+54, B0355+54, and B1929+10 are presented in § 3 and are compared to those of Brisken et al. (2002) for B0329+54 and B1929+10. We estimate the attainable astrometric accuracy at 1.4 GHz and 5 GHz in § 4 and discuss the implications of the measured distances and velocities for B1929+10 and B0355+54 in § 5.

2. OBSERVATIONS AND DATA ANALYSIS

Astrometric VLBI observations require the visibility phase of the target source to be calibrated using observations of a nearby calibrator source. Typically, the target and the "nodding" calibrator are observed in short alternate scans.

[1] Department of Astronomy, Cornell University, Ithaca, NY 14853; shami@astro.cornell.edu.
[2] National Radio Astronomy Observatory, P.O. Box O, Socorro, NM 87801.
[3] Jansky Postdoctoral Fellow.
[4] USRA, Laboratory for High-Energy Astrophysics, NASA Goddard Space Flight Center, Code 662, Greenbelt, MD 20771.
[5] Naval Research Laboratory, Code 7213, Washington, DC 20375.

To achieve phase connection across multiple scans, phase referencing requires rapid cycle times and a small angular separation between the target and the nodding calibrator (hereafter referred to as the "calibrator throw"). The limiting source of astrometric error is typically the uncalibrated differential atmosphere between the target and the calibrator, which includes an ionospheric dispersive phase error ($\propto \nu^{-1}$) and a tropospheric nondispersive phase error ($\propto \nu$). These two error terms are comparable in size at the 5 GHz band and provide an overall approximate minimum error, making the band well suited for astrometry. For example, a 0.36 mas parallax has been measured for Sco X-1 by Bradshaw, Fomalont, & Geldzahler (1999) at 5 GHz. We chose three pulsars, B0329+54, B0355+54, and B1929+10, which have flux densities between 1 and 10 mJy at 5 GHz, and observed them for seven epochs separated by 4 months each between 2000 March and 2002 March. A solar maximum occurred within this period, leading to heightened ionospheric activity and increases of $\sim$3–10 times in the daily average total electron content compared to that at solar minimum as measured by GPS (e.g., Warnant & Pottiaux 2000). Such ionospheric activity is expected to cause epoch-dependent systematic errors in our astrometry.

In each epoch, the pulsars were phase-referenced to extragalactic sources included in the International Celestial Reference Frame. B0329+54 and B0355+54 were phase-referenced to ICRF J035929.7+505750 (NRAO 150), from which they are separated by $5\overset{\circ}{.}3$ and $3\overset{\circ}{.}3$, respectively. For B1929+10, ICRF J192840.8+084848, a calibrator $2\overset{\circ}{.}3$ away, was used as a reference source, and each observation included a few scans on ICRF J193435.0+104340 (hereafter J1934+1043), only $0\overset{\circ}{.}6$ from the pulsar. The absolute positions of the calibrator sources are known to between 2–3 mas (Ma et al. 1998). The observations alternated between 90 s on the calibrator and 150 s on the target, and the pulsar gate was applied to the data at the VLBA correlator. Gating boosted the signal-to-noise ratio (S/N) by $f^{-1/2}$, a factor of $\sim$3–4, where $f = T_{\rm on}/(T_{\rm on} + T_{\rm off})$ is the gate duty cycle. AIPS, the Astronomical Image Processing System, was used for the data reduction, which followed standard procedures (Beasley & Conway 1995). The basic steps include flagging of bad records, amplitude calibration based on the system temperatures at each antenna, fringe fitting, and several passes of self-calibration on the nodding calibrator. The multiple self-calibration passes serve to correct the visibility phases and gains while fixing the position of the nodding calibrator.

For B0329+54 and B0355+54, the calibration solutions derived for the nodding calibrator were transferred to the pulsar data, images were created, and the AIPS task JMFIT was used to obtain astrometric positions at each epoch. As described by Chatterjee et al. (2001), position uncertainties were derived as a combination of the synthesized beam resolution and systematic errors in quadrature, where the systematic errors were estimated at each epoch using the deviation of the deconvolved image from that expected for a point source. While the typical uncertainties are less than 1 mas, the systematic errors were worse for B0329+54 at every epoch and exceeded 5 mas at one epoch (2000 November, because of ionospheric activity) for both pulsars, rendering that epoch useless for astrometry.

For B1929+10, after transferring the calibration solutions from the nodding calibrator, images were created for both the pulsar and the second reference source J1934+1043, and JMFIT was used as above. Ideally, a constant position should be obtained for J1934+1043 at each epoch, but the observed position varied randomly, with a median angular scatter (i.e., the median of the angular position offsets) of 0.7 mas over seven epochs. Phase self-calibration of J1934+1043 fixes its position at the expected location, and transferring these solutions to B1929+10 not only shifts the observed pulsar position but also improves the image quality and reduces the estimated systematic errors significantly. Thus, the astrometric positions for B1929+10 were referenced to J1934+1043, $0\overset{\circ}{.}6$ away. Here, too, position uncertainties at one epoch (2001 March) exceeded 5 mas, and we discarded data from that epoch in the final astrometric fits.

3. PARALLAXES AND PROPER MOTIONS

The derived positions and position uncertainties for each pulsar at 5 GHz were used to fit an annual trigonometric parallax, along with zero-point position offsets and proper motions in each coordinate (five parameters), using a weighted least-squares analysis. For B0329+54 and B1929+10, positions measured by Brisken et al. (2002) at 1.4 GHz were also used to perform joint fits; two independent zero-point position offsets were employed in the two data sets to account for the different nodding calibrators and observing frequencies. We describe the results for each pulsar in turn.

For B0329+54, unmodeled systematic errors dominate the fit and no satisfactory solution was obtained. The formal value of the parallax is $\pi = -0.45 \pm 0.36$ mas, with a reduced $\chi^2 = 2.1$ for 7 degrees of freedom. Holding the parallax fixed at 0 does not improve the fit for proper motion, yielding $\mu_\alpha = 16.8 \pm 0.4$ mas yr^{-1}, $\mu_\delta = -11.1 \pm 0.9$ mas yr^{-1}, and a reduced $\chi^2 = 2.3$ (8 degrees of freedom). Given the position uncertainties, we estimate an upper limit on the parallax of $\pi < 1.5$ mas, which is consistent with the Brisken et al. (2002) value of 0.94 ± 0.11 mas. In a joint fit to both data sets, the larger position uncertainties for the 5 GHz data leave the earlier parallax unimproved. The joint proper motion is also within the errors of the earlier Brisken et al. (2002) values of $\mu_\alpha = 17.00 \pm 0.27$ mas yr^{-1} and $\mu_\delta = -9.48 \pm 0.37$ mas yr^{-1}. The 5 GHz data do not contribute useful astrometry in this case, because the calibrator was too far away ($5\overset{\circ}{.}3$) to adequately correct phase perturbations in the data, as we discuss below.

The position uncertainties are better behaved for B0355+54 and a good weighted least-squares fit was obtained for the parallax and proper motion, with a reduced $\chi^2 = 0.82$ for 7 degrees of freedom. The derived best-fit values are listed in Table 1 and imply most probable values of $1.04^{+0.21}_{-0.16}$ kpc and 61^{+12}_{-9} km s^{-1} for the distance and the velocity, as listed in Table 2. Figure 1 shows the residual position offsets in each coordinate after subtracting the best fit proper motion, with sinusoids corresponding to the best fit parallax overplotted. It is apparent from the figure that the residual scatter in declination is significantly worse than that in right ascension. The angular separation between the calibrator and the pulsar is primarily in declination ($\Delta\alpha_{\rm cal} = 0\overset{\circ}{.}1$, $\Delta\delta_{\rm cal} = 3\overset{\circ}{.}3$), which may explain the excess scatter. Our estimates of position uncertainty do not currently account for the asymmetric calibrator throw, an issue we return to in § 4. In tests of the fit after dropping one epoch at a time, the obtained parallaxes range from $\pi = 0.87$ mas to 1.02 mas, attesting to the robustness of the reported value of 0.91 ± 0.16 mas for the parallax.

For B1929+10 as well, a good fit was obtained with a reduced $\chi^2 = 1.06$ for 7 degrees of freedom; the best-fit values are listed in Table 1. The longer time baseline of the 5 GHz data (2 yr compared to 0.77 yr for the 1.4 GHz data) results in

TABLE 1
MEASURED POSITIONS, PROPER MOTIONS, AND PARALLAXES

Pulsar	α_{J2000}[a]	δ_{J2000}[a]	μ_α (mas yr^{-1})	μ_δ (mas yr^{-1})	π (mas)
B0355+54.....	03 58 53.71650	+54 13 13.7273	9.20 ± 0.18	8.17 ± 0.39	0.91 ± 0.16
B1929+10.....	19 32 13.94970	+10 59 32.4198	94.03 ± 0.14	43.37 ± 0.29	2.76 ± 0.14
B1929+10 joint.....	19 32 13.94969	+10 59 32.4203	94.09 ± 0.11	42.99 ± 0.16	2.77 ± 0.07

NOTE.—Units of right ascension are hours, minutes, and seconds, and units of declination are degrees, arcminutes, and arcseconds.
[a] Absolute positions extrapolated to epoch 2000.0 are accurate to ~5 mas, which includes the uncertainties in the fit position and extrapolation based on proper motion (~1 mas), as well as absolute position uncertainties (<3 mas) for the ICRF sources used in phase referencing.

a more accurate proper motion determination and yields a parallax $\pi = 2.76 \pm 0.14$ mas, which differs from the Brisken et al. (2002) value of 3.02 ± 0.09 mas at the 2 σ level. The covariances between (μ_α, μ_δ) and π are (−0.37, −0.01) for the 5 GHz fit, much lower values compared to (0.79, 0.32) for the 1.4 GHz data. A joint fit to both data sets yields a parallax that is essentially unchanged from the 5 GHz value, but with smaller errors: $\pi = 2.77 \pm 0.07$ mas, with a reduced $\chi^2 = 0.97$ for 15 degrees of freedom and covariances (0.15, 0.14) between (μ_α, μ_δ) and π. The zero-point offsets for the two data sets are expected to differ since they are referenced to different nodding calibrators at different frequencies (J1945+0952 at 1.4 GHz and ICRF J192840.8+084848 at 5 GHz), but we obtain exceptionally good agreement. For the best joint fit, the difference in the zero-point offsets ($\Delta\alpha = 0.6$ mas, $\Delta\delta = 2.4$ mas) implies that the *absolute* positions agree to ~2.5 mas. The residual position offsets after subtracting the best-fit proper motion are shown in Figure 2 with the best fit parallax overplotted. The most probable value of the distance is $0.361^{+0.010}_{-0.008}$ kpc, and the velocity is 177^{+4}_{-5} km s^{-1}. Table 2 summarizes these and other derived parameters, and we defer a discussion of the ramifications of these measured parameters to § 5. The joint fits reported here are robust compared to previous measurements reported for the same pulsar (Table 3), and the gradual convergence of the measurements is also gratifying.

4. ESTIMATING ASTROMETRIC ACCURACY

In phase-referenced observations, the phases of the target visibilities are inferred from those of the nodding calibrator. For each antenna, fluctuations in the ionosphere and troposphere are sampled on an angular scale equal to the separation between the target and calibrator sources. The level of fluctuation is characterized by the phase structure function of the atmosphere (see, e.g., Thompson, Moran, & Swenson 2001, § 13.1 and § 13.3). For VLB arrays, the atmosphere is quite different at each antenna, and the uncalibrated differential phase for each visibility, which is a baseline-dependent quantity, cannot be interpreted as a simple excess in ionospheric path length or water vapor column density. It is reasonable, however, to expect that the effectiveness of phase referencing in calibrating target visibilities (and thus the quality of target images) depends on the angular separation between the target and the calibrator over which phase solutions have to be extrapolated. The temporal separation between scans on the calibrator and target introduces the time variability of the atmosphere as another source of error, but this is modest in comparison, especially for short cycle times when phase connection is achieved across multiple scans.

For the 5 GHz observations described here, B0329+54 and B0355+54 shared the same nodding calibrator, and scans on the two pulsars were interleaved in time. But as described in § 3, the quality of astrometry differed markedly for the two, leading to no useful result for one and a good submilliarcsecond parallax for the other. The primary source of error is the 5.°3 calibrator throw for B0329+54, as compared to only 3.°3 for B0355+54. The observed position for the calibrator source J1934+1043 also varied when phase-referenced to the nodding calibrator 2.°4 away, while the positions for B1929+10 were well modeled by a proper motion and parallax after referencing to J1934+1043, 0.°6 away. We quantify the random astrometric error for each pulsar at each epoch by subtracting the best-fit proper motion and parallax model and combining the residuals for each coordinate in quadrature. The median error for each of the three target pulsars is plotted against calibrator throw in Figure 3, along with the angular position scatter for J1934+1043 about the median position. In each case, the central 50% range of the estimates is indicated with error bars. We note that this plot includes just seven epochs, observed at only two declinations and three Sun angles, with potentially unusual ionospheric activity at some epochs due to solar maximum. However, the trend of increasing median errors with calibrator throw is immediately apparent for the 5 GHz data.

For comparison, we also show astrometric data at 1.4–1.6 GHz from prior projects. The parallax of PSR B0919+06 has been measured using in-beam calibration (Chatterjee et al. 2001), effectively using a calibrator throw of only 0.°2. The median residual random error, measured as above, is ~0.5 mas. The parallaxes of circumstellar masers have been measured by Vlemmings et al. (2003) using standard phase referencing at 1.6 GHz, and the median residual errors range between 1–3 mas.

TABLE 2
DERIVED PARAMETERS

Pulsar	DM (pc cm^{-3})	Distance (kpc)	D_{NE2001} (kpc)	$V_\perp$ (km s^{-1})	$\langle n_e \rangle$ (cm^{-3})
B0355+54.....	57.14	$1.04^{+0.21}_{-0.16}$	1.45	61^{+12}_{-9}	0.052
B1929+10.....	3.176	$0.361^{+0.010}_{-0.008}$	0.33	177^{+4}_{-5}	0.0087

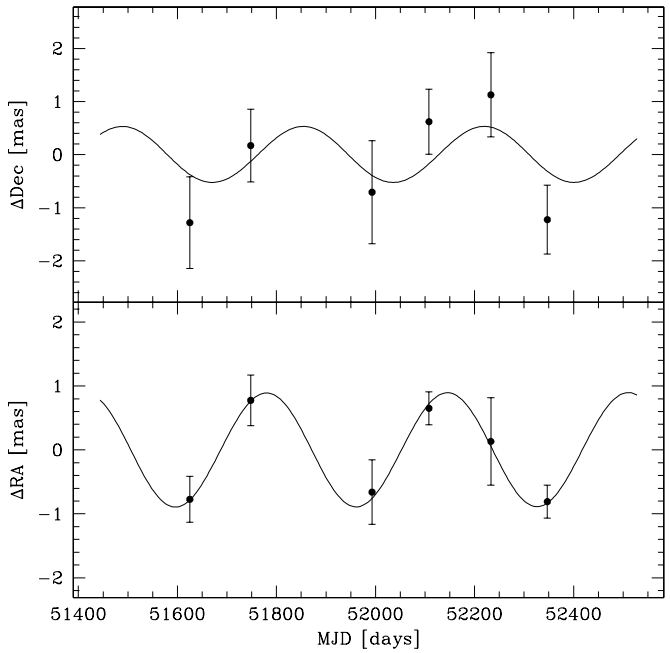

FIG. 1.—Parallax signature of PSR B0355+54 in right ascension and declination after subtracting the best-fit proper motion from the astrometric positions. Sinusoids corresponding to the best-fit parallax $\pi = 0.91$ mas are overplotted.

The median errors are indicated in Figure 3 with filled squares, along with error bars showing the inner 50% range. In addition, Vlemmings et al. (2003) performed relative astrometry between calibrator pairs, and we indicate the measured median relative scatter with outlined squares. Caveats similar to those listed for the 5 GHz data also apply here, since there are only between 4 and 12 epochs used for each measurement. As in the case of the 5 GHz data, though, the astrometric error at 1.6 GHz generally increases with increasing calibrator throw. The errors are also significantly higher than those measured at 5 GHz for comparable calibrator throws.

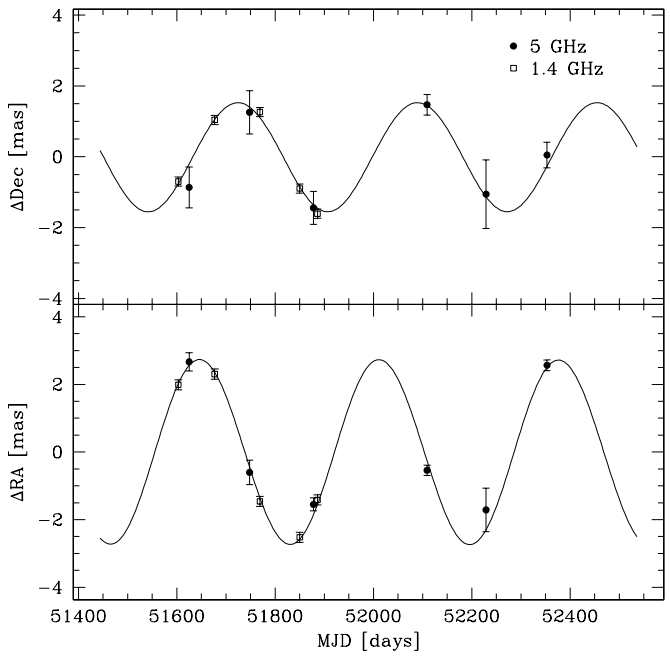

FIG. 2.—Parallax signature of PSR B1929+10 in right ascension and declination after subtracting the best-fit proper motion from the astrometric positions measured at 5 GHz (*filled circles*; this work) and 1.4 GHz (*open squares*; Brisken et al. 2002). Sinusoids corresponding to the best-fit parallax $\pi = 2.77$ mas are overplotted.

Figure 3 empirically demonstrates the potential superiority of ordinary phase-referenced astrometry at 5 GHz and emphasizes the need for additional techniques such as in-beam calibration (Fomalont et al. 1999; Chatterjee et al. 2001) or wide-band ionospheric calibration (Brisken et al. 2000) to obtain higher astrometric accuracy at lower frequencies. In § 3, we noted that the position errors for B0355+54 in each dimension ($\Delta\alpha$, $\Delta\delta$) appeared to be correlated to the calibrator throw in that dimension ($\Delta\alpha_{\rm cal}$, $\Delta\delta_{\rm cal}$). This trend is observed for all of the objects in Figure 3 at both 1.4 and 5 GHz. While the errors ($\Delta\alpha$, $\Delta\delta$) are unlikely to be completely independent of each other, the calibrator throw in each dimension is apparently an important predictor of the accuracy attainable in that dimension. Large programs now under way will provide data on astrometric precision at currently unsampled calibrator throws as well as sampling a range of Sun angles and a larger span of the solar cycle, enhancing the utility of future versions of this plot both as an observation planning tool and as a probe of the tropospheric and ionospheric structure functions. Meanwhile, the current results reiterate the importance of using the smallest possible calibrator throw in phase-referenced observations. In addition, based on these and other recent results (Chatterjee et al. 2001; Brisken et al. 2002), we predict that parallaxes and proper motions should be measurable for the majority of pulsars within 2 kpc, and even for some out to $\sim$3 kpc, using either observations at 5 GHz or lower frequency observations with additional calibration techniques. Beyond this distance range, the required precision may run up against the limits imposed by potential calibrator source structure and variability at the 100 μas level.

5. IMPLICATIONS: B0355+54 AND B1929+10

The measured parallaxes and proper motions for B1929+10 and B0355+54 lead to estimates of the distance (D) and velocity perpendicular to the line of sight ($V_\perp$) for each pulsar. The most probable values for D and $V_\perp$ and the most compact 68% probability intervals are summarized in Table 2. The distance estimated from the dispersion measure [$\mathrm{DM} = \int_0^D n_e(s)\, ds$] using the NE2001 model (Cordes & Lazio 2002) is listed for comparison. This model already includes a distance constraint for B1929+10 based on the Brisken et al. (2002) parallax and overestimates the measured distance to B0355+54 by $\sim$40%. Table 2 also lists the average electron density integrated over the line of sight, which is given simply by DM/D. The large difference between the two lines of sight reflects the complex structure in the local interstellar medium, as discussed, for example, by Toscano et al. (1999) and Cordes & Lazio (2002).

The structure of the local interstellar medium also affects the scattering properties of the pulsar signal, and measured scattering parameters can be used to constrain the distribution of scattering material along the line of sight (e.g., Chatterjee et al. 2001). Preliminary investigations suggest that the scattering properties of B1929+10 are affected by interstellar material that may be located quite close to the solar system. However, the velocity of the Earth is not negligible compared to the measured velocities of B1929+10 and B0355+54, and we postpone a detailed analysis of the interstellar scattering properties of these pulsars to future work.

TABLE 3
MEASURED PARALLAXES FOR B1929+10

Band (GHz)	π (mas)	Reference
0.4	21.5 ± 0.3	1
2.7	<4	2
2.2	5.0 ± 1.5	3
1.4	3.02 ± 0.09	4
5	2.76 ± 0.14	5
1.4, 5[a]	2.77 ± 0.07	4, 5

[a] Joint fit.

REFERENCES.—(1) Salter, Lyne, & Anderson 1979; (2) Backer & Sramek 1982; (3) Campbell 1995; (4) Brisken et al. 2002; (5) this work.

The astrometric results discussed here also lead us to reexamine, in turn, the birth site for B1929+10 based on its kinematics, the nature of its observed X-ray emission, and constraints on the cooling curve for each of the two neutron stars.

5.1. *The Birth Site of B1929+10*

Based on numerical simulations, Hoogerwerf et al. (2001) have suggested that PSR B1929+10 (which they refer to as J1932+1059) and the runaway O star ζ Ophiuchi were part of a binary system that became unbound when the pulsar progenitor exploded in a supernova $\sim$1 Myr ago in the Upper Scorpius subgroup of the Sco OB2 association. They attribute the kick velocity of the pulsar and the large space velocity of ζ Oph ($\sim$20 km s^{-1}) to the same supernova-induced binary disruption event. As seen in Figures 4 and 5 of Hoogerwerf et al. (2001), only a limited region in the parameter space of pulsar parallax, proper motion, and radial velocity allows the pulsar and ζ Oph to approach within 10 pc of each other and 10 pc of the center of the Upper Scorpius association. For these successful simulations (0.14% of the total), the implied kinematic age of B1929+10 is $\sim$1 Myr, which is comparable to its spin-down age of 3 Myr.

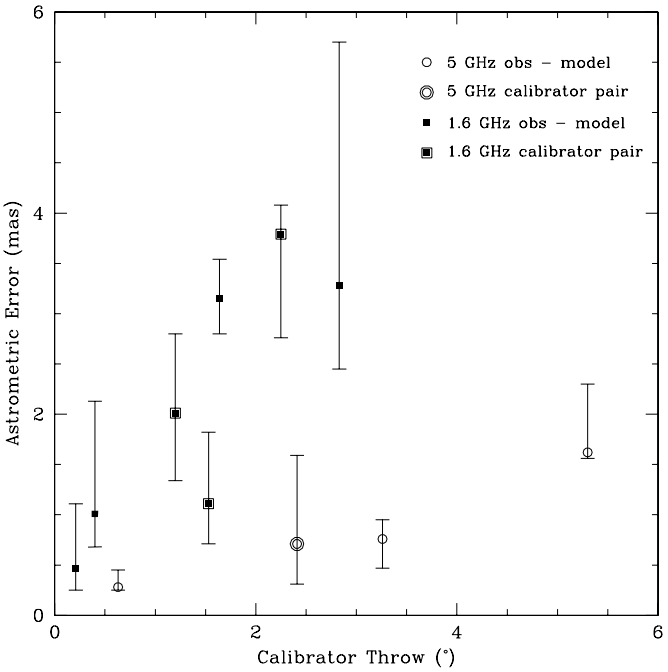

FIG. 3.—Astrometric position errors as a function of the angular separation between the target and the calibrator source. The points indicate the median scatter in the position of one calibrator measured with respect to another (*outlined symbols*), or the offset of an astrometric target position from that predicted by the best-fit proper motion and parallax model. The error bars indicate the inner 50% of the range in the scatter, between the first and third quartile. The 5 GHz data (*open circles*) are from this work. The 1.6 GHz data (*filled squares*) include results from in-beam calibration for PSR B0919+06 (leftmost point; Chatterjee et al. 2001) and VLBI astrometry of circumstellar OH masers (Vlemmings et al. 2003). There are between 4 and 12 samples at each calibrator throw, limiting the statistical significance of this plot at present, but the increase in astrometric error with calibrator throw is an unmistakable trend. Astrometric accuracy in phase-referenced observations is also better for 5 GHz data compared to 1.6 GHz data.

The distance and velocity measurements underpinning such a birth scenario are based on a "dearth of data" (Campbell 1995), and the new values for the proper motion and parallax of B1929+10 that we report here make the scenario extremely unlikely. For $\pi = 2.76$ mas, a high radial velocity ($\gtrsim$300 kms^{-1}) is required, while our proper motion measurements are inconsistent with the parameters used in the successful simulations by more than 10 σ. Therefore, B1929+10 is probably not the former binary companion of ζ Oph. We note, however, that the origin of the pulsar in the Upper Scorpius region is not excluded, and the pulsar could still have had its birth in a supernova in this region 1–2 Myr ago (de Geus 1992). The isolated neutron star RX J1856.5−3754 had initially been proposed as a potential binary companion to ζ Oph in the Upper Scorpius association (Walter 2001), but the revised distance to the neutron star (Kaplan, van Kerkwijk, & Anderson 2002; Walter & Lattimer 2002) rules this scenario out, since the closest approach by RX J1856.5−3754 to the association center occurred only $\sim$0.5 Myr ago. Thus, for ζ Oph, the alternative birth scenario in the Upper Centaurus Lupus subgroup 2–3 Myr ago (van Rensbergen, Vanbeveren, & de Loore 1996) looks more plausible.

5.2. *The Nature of X-Ray Emission from B1929+10*

X-ray emission from PSR B1929+10 was detected in observations with the *Einstein* (Helfand 1983), *ROSAT* (Yancopoulos, Hamilton, & Helfand 1994), and *ASCA* (Wang & Halpern 1997) observatories. The latter two data sets allow for spectral analysis that can be used to constrain properties of the X-ray emitting region. Yancopoulos et al. (1994) fit the *ROSAT* data to a model for blackbody emission, deriving a temperature of roughly 3×10^6 K (hereafter, 1 MK $\equiv 10^6$ K). From *ASCA* SIS data, Wang & Halpern (1997) find comparably successful fits to a single blackbody ($T = 5.14 \pm 0.53$ MK) and to a power-law spectrum. Finally, Wozna, Kuiper, & Hermsen (2003) perform spectral fits to combined *ROSAT* and *ASCA* data (using in this case the *ASCA* GIS detector) spanning the energy range 0.1–10 keV; they find acceptable fits to model spectra consisting of either a single power law or two blackbody components with temperatures of 2 and $\sim$7 MK. New observations will be needed to ascertain whether the emission is thermal or nonthermal in nature. If thermal, the existing data alone would rule out an origin for the X-rays in "cooling" emission from the entire surface of the neutron star, both because the implied temperature is unexpectedly high for such an old pulsar (characteristic age $\sim$3 Myr) and because the emitting area would be implausibly small. Indeed, as discussed by Wang & Halpern (1997), the inferred emitting area is nearly 2 orders of magnitude smaller than theoretical predictions even for the size of a heated polar cap assuming a purely dipolar star-centered magnetic field. Wang et al. (1998) elaborate on this finding, arguing that a small observed cap size may be evidence for a low heating current from the magnetosphere or an off-center dipolar

geometry, perhaps as a result of crustal plate motion on the neutron star surface.

The implications of a new distance determination depend on whether the emission from the neutron star is thermal or nonthermal in nature. If the emission is assumed to be thermal, and accurately represented by the single-blackbody result of Wang & Halpern (1997), our new distance measurement implies a bolometric luminosity[6] $L = (2.74 \pm 0.37) \times 10^{30}$ ergs s^{-1}, and an emitting area $A = (6.8 \pm 3.0) \times 10^7$ cm^2, where formal 1 σ statistical uncertainties in spectral fitting (i.e., neglecting possible systematic effects due to calibration uncertainties) and distance have been propagated and isotropic emission over 4π sr has been assumed. The new parallactic distance does not, by itself, alleviate the apparent discrepancy between observed and expected polar cap sizes, increasing the inferred emitting area by only a factor of $(361/250)^2 \simeq 2$.

Alternatively, the thermal fits of Wozna et al. (2003), to *ROSAT* and *ASCA* data simultaneously, imply emission luminosities of $L_1 = (1.85 \pm 0.30) \times 10^{30}$ ergs s^{-1} and $L_2 = (1.72 \pm 0.30) \times 1029$ ergs s^{-1}, with areas $A_1 = (1.88 \pm 0.35) \times 10^9$ cm^2 and $A_2 = (1.34 \pm 0.36) \times 10^6$ cm^2 for the 2 MK and 7 MK blackbody components, respectively. If this spectral model holds, the intrinsic emitting area of the low-temperature component,

$$A_1^{\rm int} = A_1(1 - 2GM/Rc^2) = 1.1 \times 10^9 \ {\rm cm}^2, \qquad (1)$$

comes within a factor of 3 of the canonical polar cap size defined by the last open field lines in the pulsar magnetosphere,

$$A_{\rm pc} = \frac{2\pi^2 R^3}{cP} = 2.9 \times 10^9 \ {\rm cm}^2, \qquad (2)$$

where P is the pulse period. This similarity is intriguing given uncertainties in magnetospheric geometry, the beaming solid angle, and likely distortion of the surface blackbody spectrum due to propagation of the radiation through a stellar atmosphere.

If, instead, the observed X-ray emission is interpreted correctly by the nonthermal model of Wozna et al. (2003), then the 0.1–10 keV luminosity implied by our new distance measurement is $L_{\rm PL} = (9.6 \pm 0.8) \times 10^{30}$ ergs s^{-1}. In the 2–10 keV band, the same model implies an X-ray luminosity of 3.1×10^{-4} the pulsar's spin-down power, $\dot{E}$, comparable to the nonthermal X-ray emissions of other pulsars (Possenti et al. 2002).

Finally, we address the implications of our new distance determination on stellar cooling models for B1929+10. Following the procedure adopted by Yancopoulos et al. (1994), we derive upper bounds on the surface temperature by requiring that the whole-surface "cooling" emission not exceed the observed soft-band (0.09–0.30 keV) *ROSAT* count rate. The result is sensitive to the assumed absorption column, $n_{\rm H}$. For the parallactic distance and the smallest likely $n_{\rm H}$, 1.5×10^{20} cm^{-2}, a temperature $T \lesssim 0.24$ MK is required, corresponding to a luminosity limit $L \lesssim 4 \times 10^{30}$ ergs s^{-1}, roughly an order of magnitude larger than typical theoretical expectations ($\sim 5 \times 10^{29}$ ergs s^{-1}) for residual heat retained since the formation of such an old pulsar (Tsuruta et al. 2002). If $n_{\rm H}$ is allowed to be as large as 6.5×10^{20} cm^{-2}, the 1 σ upper limit for thermal models derived by Wozna et al. (2003), an even hotter surface is allowed: $T \lesssim 0.35$ MK and $L \lesssim 2 \times 10^{31}$ ergs s^{-1}. We therefore conclude that available soft X-ray measurements of PSR B1929+10 do not usefully constrain leading cooling models.

[6] Unless otherwise noted, all luminosities, temperatures, and emitting areas are quoted for a distant observer. Where adjustments are made for redshift at the neutron star surface, canonical values $M = 1.4$ $M_\odot$ and $R = 10$ km are assumed.

5.3. *High-Energy Emission from B0355+54*

PSR B0355+54 was detected by the *ROSAT* observatory (Slane 1994). Too few photons were acquired to permit detailed spectral modeling, but the gross distribution of photon energies suggested nonthermal emission. A recent observation with the *XMM-Newton* telescope has confirmed this conclusion (J. Kennea et al. 2004, in preparation). Adopting a distance of 2.1 kpc, Slane (1994) inferred a nonthermal luminosity (0.1–2.4 keV) of 1.0×10^{32} ergs s^{-1}; scaling to the parallactic distance of 1.04 kpc results in a revised luminosity of 2.4×10^{31} ergs s^{-1}. The available *XMM-Newton* data also provide a 1 σ upper bound on the surface cooling luminosity of the neutron star, $L < 4.5 \times 10^{32}$ ergs s^{-1} (J. Kennea 2003, private communication). As with B1929+10, this limit is consistent with leading cooling models (Tsuruta et al. 2002).

The new distance measurement for B0355+54 has similar implications for studies of the γ-ray emission from the pulsar. The EGRET instrument on board *CGRO* set an upper limit to the flux of 0.1–10 GeV photons that implies a conversion efficiency $\eta_\gamma \equiv L_\gamma/\dot{E} < 0.2$ (Nel et al. 1996) if the γ-ray beam crosses the line of sight. Our parallactic distance, nearly a factor of 2 smaller than the dispersion-derived distance, further reduces the apparent γ-ray efficiency, $\eta_\gamma < 0.05$, placing B0355+54 at odds with the observed trend of increasing η_γ with spin-down age. For example, PSR B1055−52, with a characteristic age similar to B0355+54, has $\eta_\gamma \simeq 0.7$. If the trend of γ-ray efficiency increasing with age holds, the likely conclusion is that the γ-ray beam for B0355+54 does not cross our line of sight, as predicted in the outer-gap beaming model of Yadigaroglu & Romani (1995).

6. CONCLUSIONS

We have presented results from VLBA astrometric observations of three pulsars at 5 GHz. For B0329+54, the systematic errors are large enough that we obtain only an upper limit to the parallax, $\pi < 1.5$ mas, and proper motions consistent with the Brisken et al. (2002) value. The large angular separation between the calibrator and pulsar (5.°3) is the most probable cause for the large systematic errors. With the same calibrator and at the same observation epochs, but with a smaller angular throw (3.°3), we obtain a proper motion and parallax for B0355+54, with an implied $D = 1.04^{+0.21}_{-0.16}$ kpc and $V_\perp = 61^{+12}_{-9}$ km s^{-1}.

For B1929+10, we demonstrate the consistency of our absolute astrometry with that of Brisken et al. (2002) to within $\sim$2.5 mas. The longer time baseline of the 5 GHz data permits a better proper motion measurement while reducing the covariance between μ and π. A joint fit to both data sets produces a parallax identical to that measured with the 5 GHz data alone (but with smaller uncertainties), implying a distance $D = 0.361^{+0.010}_{-0.008}$ kpc and velocity $V_\perp = 177^{+4}_{-5}$ km s^{-1}. The results for B1929+10 illustrate the need for both a time baseline long enough to minimize the covariance between μ and π and a sufficient number of epochs so that the parallax signature is well sampled.

Based on the observed astrometric errors in our observations, as well as the astrometric uncertainties measured by Chatterjee et al. (2001) and Vlemmings et al. (2003) at

1.4 GHz, we quantify the astrometric error as a function of calibrator throw and observing frequency. The astrometric precision is correlated with the angular throw between the calibrator and the target, with lower errors at 5 GHz compared to 1.4 GHz. Figure 3 provides a first attempt at quantifying this dependence on an empirical basis, although we note that the random nature of these errors implies that a parallax value smaller than the predicted astrometric error can still be measured given enough measurement epochs. The calibrator throw in each dimension may serve as an important predictor of the accuracy attainable in that dimension. Future observations will allow us to confirm or refute this apparent correlation.

Finally, we have investigated the implications of the new distance and transverse velocity determinations for B1929+10 and B0355+54. We conclude that B1929+10 and the runaway O star ζ Ophiuchi do not approach within 10 pc of each other when their paths are traced back in time, given the revised distance and velocity for the pulsar. Thus, contrary to the suggestion by Hoogerwerf et al. (2001), they are unlikely to have been members of a binary system that was disrupted by the birth supernova of the pulsar. A review of X-ray data allows us to constrain the luminosity of the two pulsars in soft X-rays. The limits on the thermal emission from both objects are consistent with (and unconstraining for) leading neutron star cooling models (Tsuruta et al. 2002). If the X-ray emission from B1929+10 is thermal in nature, the emitting area for X-rays is roughly consistent with the canonical size for a heated polar cap. For B0355+54, the inferred conversion of spin-down power to γ-ray luminosity is low, which may imply that its γ-ray beam does not intersect our line of sight.

The implications that we discuss here illustrate the range and diversity of the applications of new distance and velocity measurements for neutron stars. Most pulsars are weak at 5 GHz, but we expect that a few others will be observable with the VLBA alone. The addition of telescopes with large collecting areas such as Arecibo and the Green Bank Telescope to the array will allow us to further enlarge the sample and explore the consequences at multiple wavelengths.

We thank Andrew Lyne and Michael Kramer at the Jodrell Bank Observatory for pulsar timing solutions used to gate the VLBA correlator, Walter Brisken for useful discussions about the 1.4 GHz astrometric results, and Jamie Kennea for sharing results from *XMM-Newton* observations of B0355+54 prior to publication. The National Radio Astronomy Observatory is a facility of the National Science Foundation (NSF) operated under cooperative agreement by Associated Universities, Inc. This work at Cornell was supported in part by NSF grants AST 9819931 and AST 0206036 and made use of NASA's Astrophysics Data System Abstract Service and the arXiv.org astro-ph preprint service as well as data obtained from the High Energy Astrophysics Science Archive Research Center (HEASARC) provided by NASA's Goddard Space Flight Center. W. V. thanks the Niels Stensen Foundation for partially supporting his stay at Cornell University, and Z. A. acknowledges support from grant NRA-99-01-LTSA-070 to NASA GSFC. Basic research in radio astronomy at the Naval Research Laboratory is supported by the Office of Naval Research.

REFERENCES

Arzoumanian, Z., Chernoff, D. F., & Cordes, J. M. 2002, ApJ, 568, 289
Backer, D. C., & Sramek, R. A. 1982, ApJ, 260, 512
Beasley, A. J., & Conway, J. E. 1995, in ASP Conf. Ser. 82, Very Long Baseline Interferometry and the VLBA, ed. J. A. Zensus, P. J. Diamond, & P. J. Napier (San Francisco: ASP), 328
Bradshaw, C. F., Fomalont, E. B., & Geldzahler, B. J. 1999, ApJ, 512, L121
Brisken, W. F., Benson, J. M., Beasley, A. J., Fomalont, E. B., Goss, W. M., & Thorsett, S. E. 2000, ApJ, 541, 959
Brisken, W. F., Benson, J. M., Goss, W. M., & Thorsett, S. E. 2002, ApJ, 571, 906
Burrows, A., & Hayes, J. 1996, Phys. Rev. Lett., 76, 352
Campbell, R. M. 1995, Ph.D. thesis, Harvard Univ.
Chatterjee, S., Cordes, J. M., Lazio, T. J. W., Goss, W. M., Fomalont, E. B., & Benson, J. M. 2001, ApJ, 550, 287
Cordes, J. M., & Lazio, T. J. W. 2002, preprint (astro-ph/0207156)
de Geus, E. J. 1992, A&A, 262, 258
Fomalont, E. B., Goss, W. M., Beasley, A. J., & Chatterjee, S. 1999, AJ, 117, 3025
Helfand, D. J. 1983, in IAU Symp. 101, Supernova Remnants and Their X-ray Emission, ed. J. Danziger & P. Gorenstein (Dordrecht: Reidel), 471
Hoogerwerf, R., de Bruijne, J. H. J., & de Zeeuw, P. T. 2001, A&A, 365, 49
Kaplan, D. L., van Kerkwijk, M. H., & Anderson, J. 2002, ApJ, 571, 447
Lorimer, D. R., Yates, J. A., Lyne, A. G., & Gould, D. M. 1995, MNRAS, 273, 411
Ma, C., et al. 1998, AJ, 116, 516
Nel, H. I., et al. 1996, ApJ, 465, 898
Possenti, A., Cerutti, R., Colpi, M., & Mereghetti, S. 2002, A&A, 387, 993
Salter, M. J., Lyne, A. G., & Anderson, B. 1979, Nature, 280, 477
Slane, P. 1994, ApJ, 437, 458
Taylor, J. H., & Cordes, J. M. 1993, ApJ, 411, 674
Thompson, A. R., Moran, J. M., & Swenson, G. W. 2001, Interferometry and Synthesis in Radio Astronomy (2nd ed.; New York: Wiley)
Toscano, M., Britton, M. C., Manchester, R. N., Bailes, M., Sandhu, J. S., Kulkarni, S. R., & Anderson, S. B. 1999, ApJ, 523, L171
Tsuruta, S., Teter, M. A., Takatsuka, T., Tatsumi, T., & Tamagaki, R. 2002, ApJ, 571, L143
van Rensbergen, W., Vanbeveren, D., & de Loore, C. 1996, A&A, 305, 825
Vlemmings, W. H. T., van Langevelde, H. J., Diamond, P. J., Habing, H. J., & Schilizzi, R. T. 2003, A&A, 407, 213
Walter, F. M. 2001, ApJ, 549, 433
Walter, F. M., & Lattimer, J. M. 2002, ApJ, 576, L145
Wang, F. Y.-H., & Halpern, J. P. 1997, ApJ, 482, L159
Wang, F. Y.-H., Ruderman, M., Halpern, J. P., & Zhu, T. 1998, ApJ, 498, 373
Warnant, R., & Pottiaux, E. 2000, Earth Planets Space, 52, 1055
Wozna, A., Kuiper, L., & Hermsen, W. 2003, preprint (astro-ph/0302452)
Yadigaroglu, I.-A., & Romani, R. W. 1995, ApJ, 449, 211
Yancopoulos, S., Hamilton, T. T., & Helfand, D. J. 1994, ApJ, 429, 832